Laser-induced graphenization of textile yarn for wearable electronics application

Laser-induced graphenization of textile yarn for wearable electronics application

*Matteo Parmeggiani [a,b], Stefano Stassi [a], Marco Fontana [a,b], Stefano Bianco [a], Felice Catania [a], Luciano Scaltrito [a], Andrea Lamberti [a,b]**

[a] Politecnico di Torino, Dipartimento di Scienza Applicata e Tecnologia (DISAT), Corso Duca Degli Abruzzi, 24, 10129 Torino, Italy

[b] Istituto Italiano di Tecnologia, Center for Sustainable Future Technologies, Via Livorno 60, 10144 Torino, Italy

*Corresponding Author: andrea.lamberti@polito.it

KEYWORDS Laser-induced graphene; textile yarn; wearable electronics; sensors.

ABSTRACT The present paper deals with the selective laser writing of textile yarns in order to induce a conductive path useful for smart textiles application. The incident power of the laser induces a conversion of an aramid fiber surface into graphene-based conductive material with tunable electrical properties depending on the laser writing parameters. The physical-chemical properties of the resulting smart yarns have been intensively characterized by electron microscopy, Raman spectroscopy, electrical and mechanical investigations. The results confirm the few-layer graphene fingerprint of the written paths onto the textile yarn with suitable properties for their application into electronic textiles. Indeed, a yarn-shape strain sensor with excellent performance

has been developed and characterized to demonstrate the potential application of the proposed technology to the wearable electronic field.

Introduction

Laser-induced graphene (LIG) obtained by laser writing of polymeric substrates has been recently reported as an incredibly promising material for flexible electronics. [1] It consists of a three-dimensional network of few layer graphene (FLG) obtained by a laser writing process of the polymer surface.[2] In the last years it has been applied to many fields with extraordinary performance, thanks to its intrinsic properties and to the easy, fast, cost-effective and scalable fabrication process.[3-8]

Herein we focus the attention on polymeric materials in form of wires or yarns, and consequently all their machining into cloth for their application as electronic smart textiles.

The recent rapid development of wearable electronics and e-textiles has increased the need for innovative materials able to satisfy both the stringent requirements of electrical conductivity, flexibility and compatibility with textile production processes.[9] Several solutions have been proposed mainly considering a wire-shaped current collector (metal wires or carbon-based fibers).[10-13] Depending on class of wearable device (sensors, energy harvesting, energy storage, …) this kind of substrates are then covered by a functional material regarding the specific application. The coating can be performed by wet (dip-coating, sol-gel, hydrothermal or electrochemical synthesis) or dry approaches (chemico-physical depositions such as sputtering, evaporation, atomic-layer deposition, …).[14] Nevertheless, many of these coating approaches cannot provide a direct pattern, but a previous lithographic step has to be performed in order to

transfer a desired geometry. Moreover, in most of the wearable device applications porous materials are required in order to expose high surface area.

For these reasons, laser writing onto a fiber has been proposed to overcome the complexity of the lithographic steps allowing a direct patterning of some materials. For examples it has been reported to fix dye molecules or to write a coloured pattern.[15] Only few examples regarding the possibility to write conductive path have been proposed and are related to the direct laser writing of graphene oxide fibers resulting in a locally reduced graphene oxide.[16] However, this solution strongly restricts the range of materials usable for the wearable device fabrication.

Herein, we propose to laser write the polymeric yarns in order to induce graphene-based paths (see **Scheme 1**) in a direct patterning step, avoiding the need of a current collector and deeply simplify the device fabrication process. Aramid has been selected as yarn material since it represents a very good candidate for laser graphitization thanks to its aromatic structure (see inset of Scheme 1), it exhibits excellent resistance and toughness, and it can be considered an effective case of study for future real application since many aramid-technical textile could take advantage from the integration of flexible electronics (e.g. flame retardant, anti-cut, bulletproof and industrial use clothing).[17-19]

The writing process has been optimized to *i*) maximize the electrical conductivity, *ii*) avoid yarn ablation and *iii*) preserve at the same time suitable mechanical properties for its further exploitation as e-textile application. Finally, a yarn-shape strain sensor has been fabricated to demonstrate the potentiality of the proposed approach for wearable electronics achieving promising deformation sensing capability.

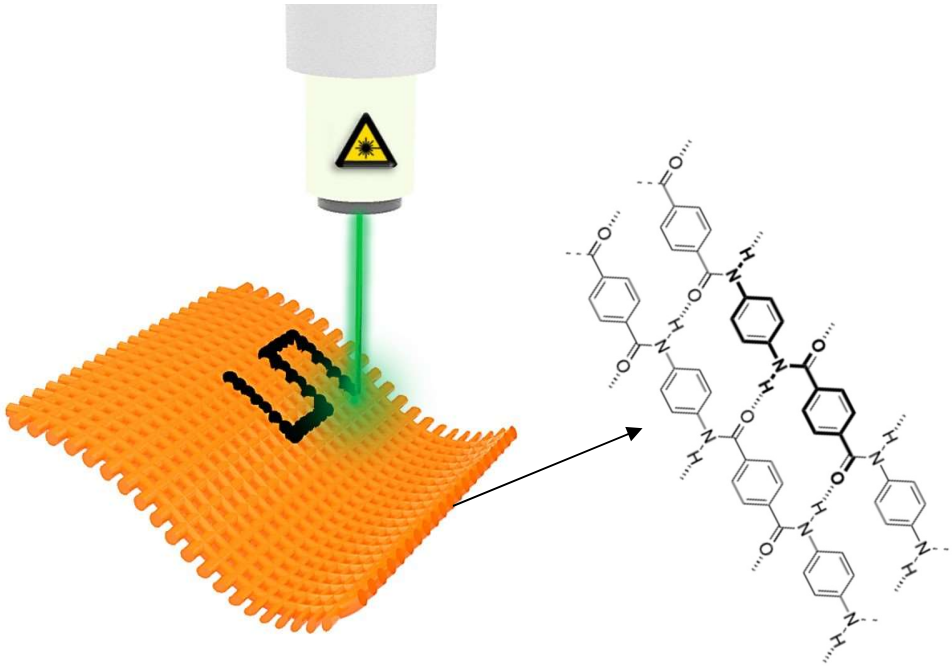

Scheme 1. Laser-induce conductive path on aramid yarns for e-textile application.

Experimental

Laser writing setup

The laser writing of polymer yarns has been performed using an Ytterbium doped femtosecond laser source (Microla Optoelectronics Srl, **Figure S1**a) where the second emission harmonic at $\lambda = 514\ nm$ has been exploited, with pulse width of 214 fs at a repetition rate of 100 kHz. The laser is equipped with aspheric lens with focal length f = 18.75 mm, RMS Asphere Figure Error 0.25 µm and numerical aperture 0.66. The laser beam with initial diameter of 3 mm is passed through a 2X beam expander, and the divergence of the beam after the expander is θ = 0.225 mrad. The final theoretical spot size d_0 is therefore $d_0 = \theta \cdot f = 4\ \mu m$.

An output power of 500 mW (1W on the first harmonica set on the software) and axis position scan speed of 0.5 mm/s were used to ensure the graphitization of the aramid yarn. In order to

precisely focus the beam on the wire, this was mounted on a 3D-printed holder fixed on the chuck beneath the laser head (**Figure S2**), and focus was manually set at the top surface of the yarn by means of a dedicated camera. The variable thickness of the intertwined fibers along its length frequently caused loss of focusing during the writing process, yielding a non-uniform graphitization of written path. Three different writing procedures have been developed in order to optimize the uniformity of the process. The first procedure consisted in writing a single line, 3.5 cm long, centered on the yarn and parallel to its longitudinal axis. The second scheme involved a double writing of the same 3.5 cm long line, lowering the focus by 50 μm towards the bulk of the wire between the two writing steps. The third procedure consisted in writing a rectangular area of 3 cm x 100 μm, with line spacing of 25 μm, focused on the top surface of the yarn and aligned along its longitudinal axis. The sample are named "1-line", "2-lines" and "area" in the following text.

Characterization

Scanning Electron Microscopy characterization was carried out with a field-emission scanning electron microscope (FESEM Supra 40, manufactured by Zeiss) equipped with a Si(Li) detector (Oxford Instruments) for energy-dispersive x-ray spectroscopy.

Transmission Electron Microscopy characterization was performed on a FEI Tecnai G2 F20 S-TWIN instrument operated at 200 kV acceleration voltage. Regarding sample preparation, LIG flakes were detached from the laser-treated yarn by sonication and they were subsequently dispersed in high-purity ethanol (> 99.8%). Finally, the LIG dispersion was drop-casted to a lacey carbon Cu TEM grid.

Raman spectroscopy was performed by means of a Renishaw InVia Reflex micro-Raman spectrometer, equipped with a cooled CCD camera. A 514.5 nm laser source was used, focused through a 50X microscope objective, with backscattering light collection.

Mechanical properties of the samples were tested with a Universal Testing System (Instron 3365). The piezoresistive measurements were conducted with a Keithley 2635A source meter. For the bending deformation, the samples were bended over cylinders with different radii, while for dynamic deformation the samples were mounted on a mechanical shaker (TV51110, Tira Gmbh, Germany) driven by means of a function generator and a controller (VR 9500, Vibration Research, USA) to produce a cyclic movement with the desired magnitude and period. Force and acceleration were controlled with a load cell and an accelerometer screwed on the plate of the shaker. The samples were attached to the plate and brought into compression during each cycle by pressing on a fixed steel bar placed above the shaker (scheme in Figure S5).

Results and discussion

The first main issue related to the laser writing of single yarn relies on the possibility to achieve very narrow lines of LIG. This goal has been achieved thanks to the utilization of a femtosecond laser with suitable laser parameters as described in the experimental and in the supporting information (**Table S1** and Figure S2). The second problem consists in the alignment of the laser pattern onto a 1D substrate such as the polymeric wire to be graphitized. This issue has been faced by fabricating a dedicated support shown in Figure S2 exploiting additive manufacturing technology. The laser writing of single yarn represents a quite difficult procedure since it is necessary to focus the laser spot onto a complex surface. This problem obviously implies that during laser writing some regions of the polymer surface will be defocused, strongly affecting the

local photothermal conversion of the polymer into LIG. Three different writing procedures have been implemented, to compensate the non-planarity of the substrate. The first method relies on the writing of the yarn with a single line about 40 µm wide ("1-line"), the second approach is based on the laser writing of two lines, one over the other, but lowering the focus position of 50 µm after the first writing step ("2-lines") while the third method considers an area that covers the upper surface of the yarn ("area"). The choice of the writing approach has a heavy impact on the mechanical and electrical properties of the LIG on the wire, as will be discussed later. Optical microscopy images of the three obtained samples are reported in **Figure S3**.

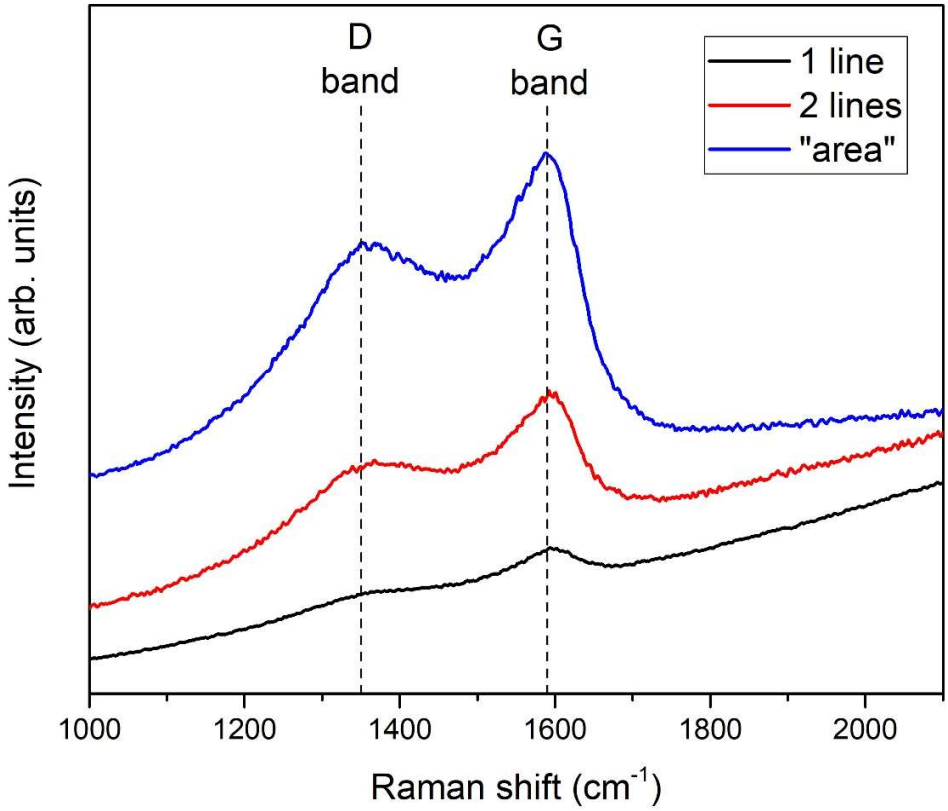

Figure 1. Typical Raman spectra of the laser-written fibers subjected to different writing procedures ("1-line", "2-lines" and "area")

As regards of the graphitization level, some important information on the chemical-physical characteristics of the material can be obtained through Raman spectroscopy. The Raman spectrum of the aramid polymeric material, is dominated by fluorescence, characterized by a light emission with energy lower than the incident light (green laser excitation at 514.5 nm), distributed in a broad spectrum, with a profile of increasing intensity with increasing wave numbers. On the other hand, when the material is graphitized, the typical D and G resonances (at about 1350 cm^{-1} and 1580 cm^{-1} respectively), characteristics of sp2 hybridized carbonaceous materials, can be revealed. From micro-Raman analysis, reported in **Figure 1**, it emerges that the typical fingerprint represented by D and G peaks is more evident for samples subjected to "area" pattern, witnessing in such case a higher graphitization degree. For single line and double line pattering, the incomplete conversion of the material is evident, resulting in a luminescence emission superimposed to the Raman spectrum. It is important to underline that micro-Raman measurements are punctual measurements, carried out through a 50X optical magnification. Consequently, the signal is related to spatial areas of samples having the characteristic size of a few tens of micrometers. The presence of graphitization within the material is therefore indicative of the effectiveness of the laser treatment produced, but does not guarantee the achievement of uniformity along the entire line, or in different areas. From the performed measurements, all in areas subject to laser treatment, different graphitization profiles are highlighted. In fact, as reported in **Figure S4**, one can notice that the signal passes from a fluorescence profile (typical of the matrix material) with a very weak graphitization imprint (point 1), to a more complete graphitization profile (point 4), with intermediate states in the middle (point 2 and point 3). The conversion of the material into a

graphitic structure is not complete as expected in a local treatment with a focused laser to obtain writing of conductive strips while maintaining the mechanical characteristics of the fabric.

A more detailed analysis of the laser writing effect on the LIG generation onto the fibers has been done by electron microscopy. **Figure 2** shows the FESEM images of the aramid yarn before and after laser irradiation with the "area" pattern.

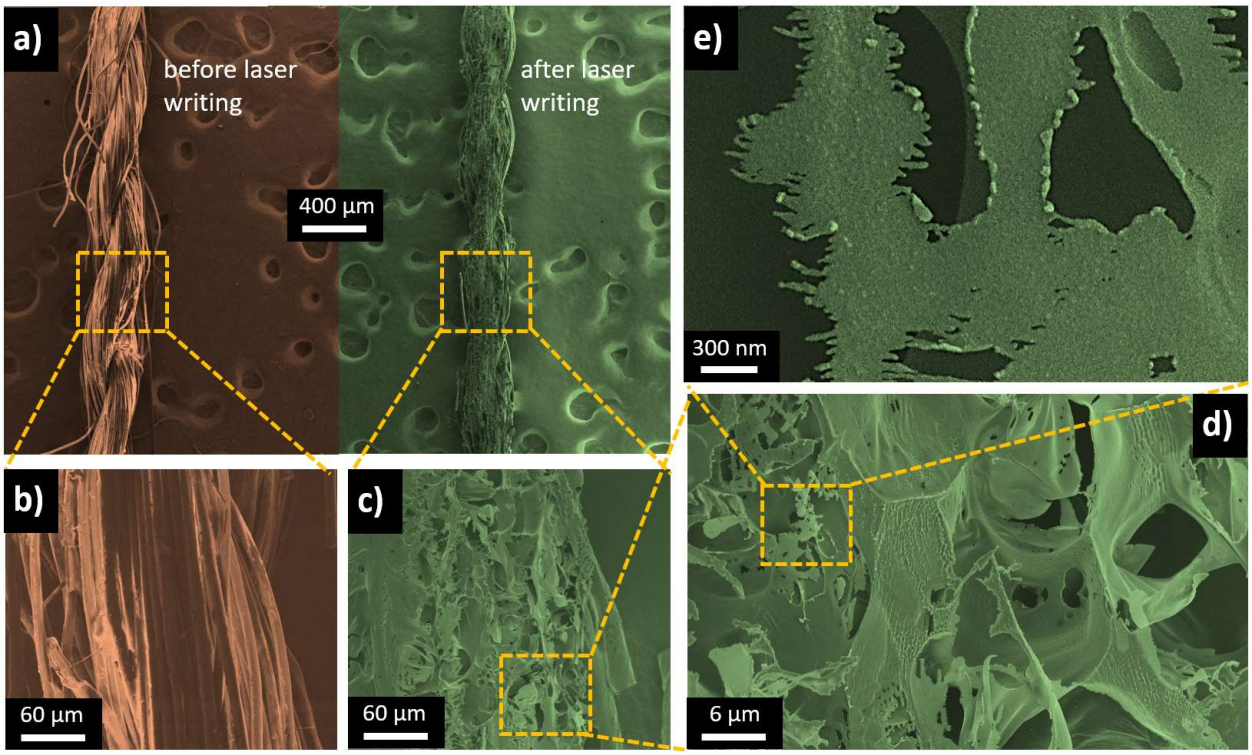

Figure 2. FESEM images of the aramid yarns before and after ("area") the laser writing (a) together with higher magnification images of the aramid filers (b) and of the obtained LIG (c-e).

The foam-like appearance is caused by the release of gas during the laser-writing process. Laser irradiation locally raises the temperature, causing chemical bonds to break and the sublimed atoms recombine into gaseous products which find their way out of the structure through the generation of bubbles and then holes.

Further confirmation of the successful graphitization of the material is obtained by Transmission Electron Microscopy (TEM) of electron transparent LIG flakes (such as the one shown in **Figure 3**a) obtained from the yarn treated with the "area" pattern.

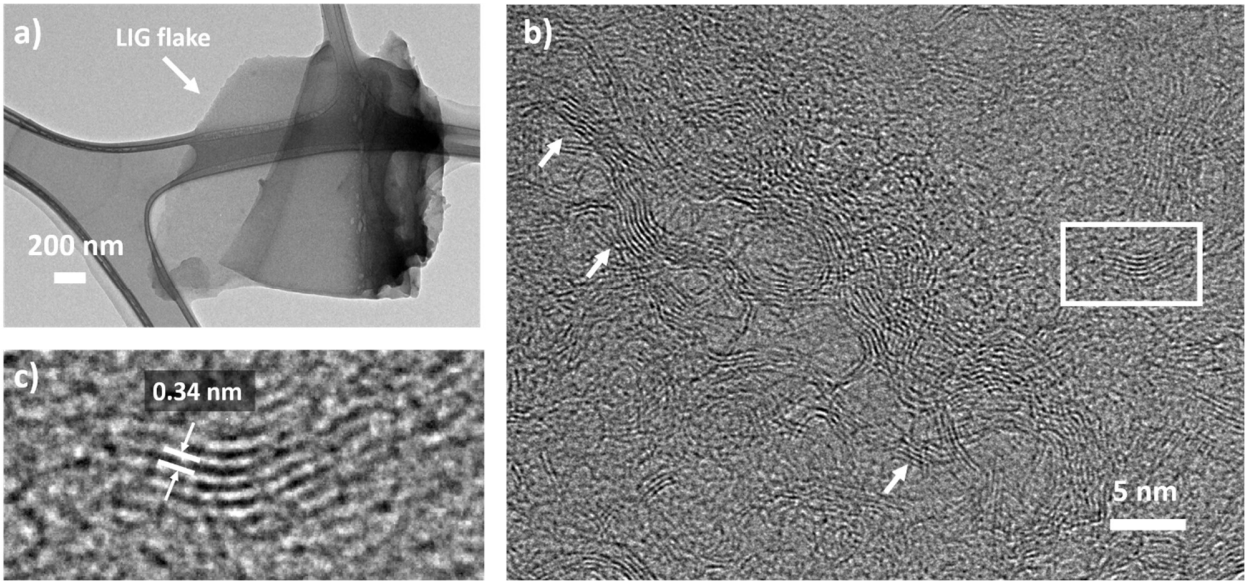

Figure 3. Low-magnification bright-field TEM image of LIG flake (a). High-magnification TEM image of a LIG flake (b) were the arrows provide indication of visible few-layer graphenic domains while the rectangular box highlights the region depicted the high-resolution image (c).

Based on high-magnification TEM images (Figure 3b), a typical structure of randomly-oriented few-layer graphene domains is present, in accordance with previously-reported LIG materials.[3-4] The domains are clearly identified in high-resolution TEM images (Figure 3c) by the characteristic ~ 0.34 nm interplanar spacing of the (002) family of planes in the graphitic structure.

Having confirmed the effectiveness of the laser writing to produce the LIG pattern on the aramid yarn, the samples were therefore electrically characterized by creating an ohmic contact through the use of a commercial silver-based conductive paste (RS, Ag-conductive paint) at the ends of the LIG lines. Micromanipulators have been used to connect the electrical contacts.

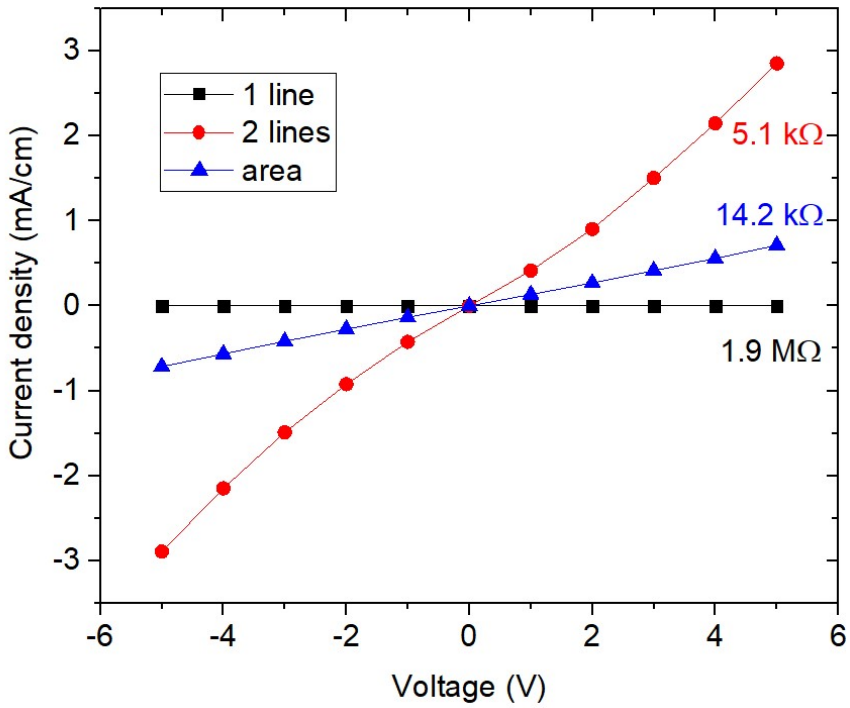

Figure 4. IV measurements of laser written aramid wires using a single line path, a double pass of the laser spot on the same line and an area.

From the results shown in **Figure 4**, the writing approach that guarantees the lowest resistance (and therefore the best conductivity) is represented by the “2-lines” technique.

The sample prepared with "area" pattern resulted less conductive than the “2-lines”, while “1-line” approach returns the most resistive samples, probably due to the discontinuous LIG pattern on the complex yarn surface.

On the counterpart the conductive properties of the “2-lines” sample (and such aspect is evident also on “1-line” samples) are preserved only on short written paths. Indeed, for path longer than few millimetres some discontinuities affect the current flow leading to open circuit problems. These can be ascribed to the complex surface of the yarn but also to the handling of the flexible sample after writing, which is easily subjected to tensile and compressive strain. Conversely, the

“area” sample can warrant good electrical properties up to several centimetres due to the higher number of electrical connections among the LIG flakes within the written path.

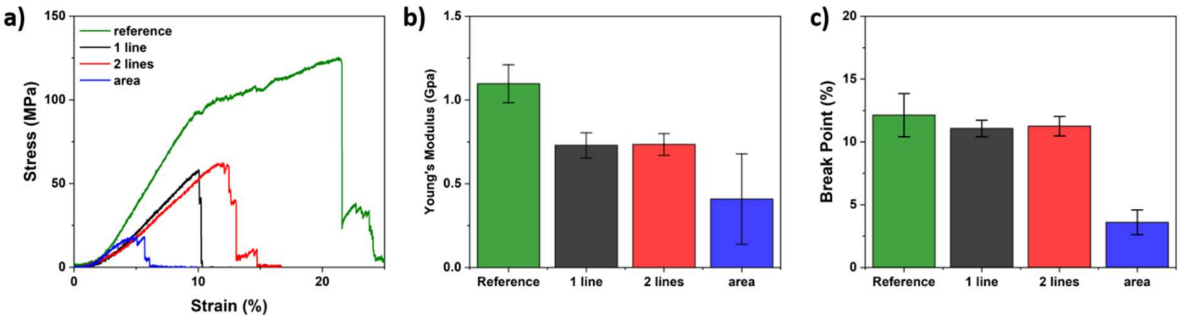

Figure 5. a) Stress-strain curves of yarns not modified with laser writing (reference) and yarns after the three different writing laser procedures. b) Young's modulus values and c) breaking point of the different yarn samples.

Concerning the mechanical performances, tensile measurements by blocking the different fibers between two grips has been performed. The fibers were put in traction by moving the grips apart at a speed of 2.5 mm/min while measuring the force applied until the fibers broke. The elastic modulus was then extracted from the slope of the initial linear section of the stress-strain curve. The breaking point represents the strain value at which a sudden change in the stress exerted on the fibers is registered. The mechanical measurements shown in **Figure 5** represent the stress-strain curves (Figure 5a), the values of the elastic modulus (or Young's modulus, Figure 5b) and the breaking point (Figure 5c) of untreated yarns and yarns laser written with the three different approaches. As it can be seen from the images, the mechanical properties of the fibers are only slightly worsened, compared to the starting fiber, when one or two writing lines are performed with the laser. Instead, there is a more marked deterioration of the mechanical properties when writing an area geometry on the fibers. However, since the “area” sample is the only one that can provide long electrically conductive path, it has been selected for further processing.

Indeed, the present findings reveal that laser written aramid yarns are sufficiently electrically conductive and mechanically stable to be used as flexible electronic device. For this reason, a first prototype has been fabricated and characterized to illustrate the possible application as yarn-shape strain sensor.

The laser-written thread was bound on a PET support by means of an adhesive polyimide tape. The Ag-paste was spread manually and let dry for about 5 minutes, then a metal wire (Goodfellow, copper wire 50 micrometers) was inserted into the semi-rigid paste to provide electrical connection for the sensor. The conductive paste was then thermally treated at 70 ° C for 1 hour in a convection oven to allow complete solidification and ensure greater stability during the measurement phase. The complete sensor composition is shown in **Figure 6**a.

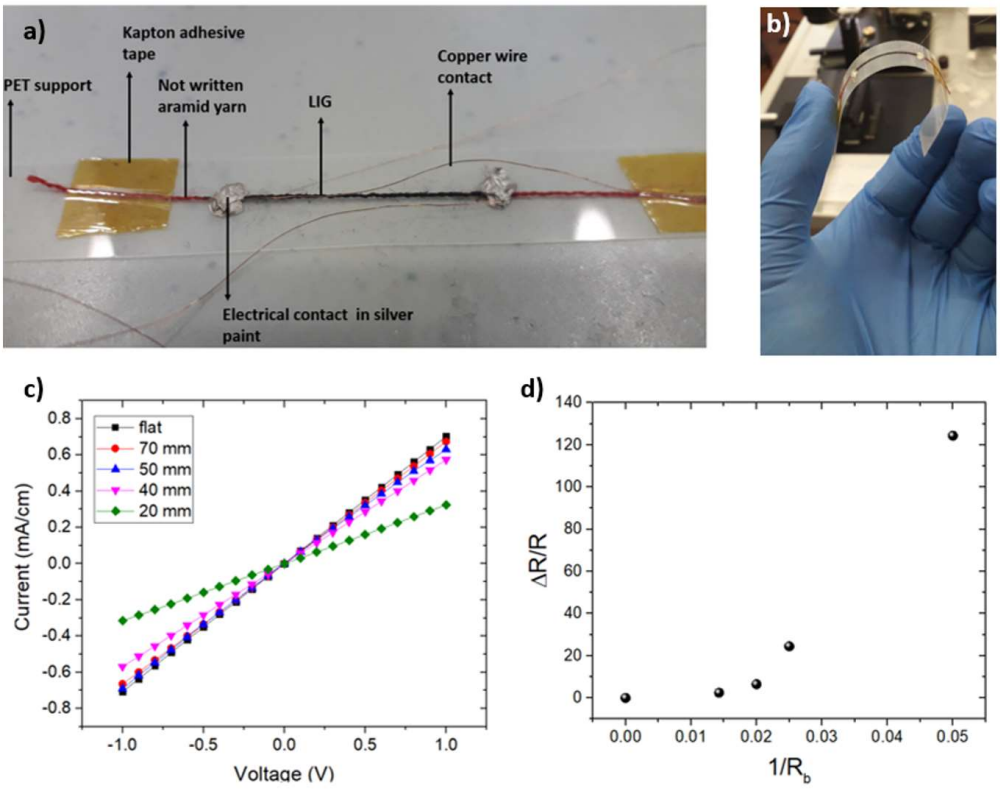

Figure 6. Digital photograph of the "LIG on yarn" deformation sensor prototype (a,b).

Voltage *vs* current characteristics of the sensor subjected to deformation with various radii of curvature (c) and relative ΔR / R values (d).

First the device was tested as flexible bending sensor by bending the wire on cylinders with different diameters and thus radius of curvature (Figure 6b-c). As can be seen from Figure 6b, the deformation of the sensor by reducing the radii of the cylinders increases its electrical resistance. When the sample is deformed, the walls of the LIG move away from each other, and therefore the percolation paths for electrons in the material decrease resulting in an increase of electrical resistance.

Subsequently, the sample was subjected to cyclic deformations in order to be able to appreciate its repeatability in a real context of use (see **Figure S5** for instrumental set-up). The measurement was performed by periodically compressing the sensor mounted on a mechanical shaker over a fixed steel bar at a fixed force measured by a force cell.[20] As can be seen from **Figure 7**a, the electrical resistance of the yarn sensor varies according to the shape of the applied force. The sensor is very sensible to small forces and a resistance variation up to 10% is registered for forces of the order of few tens of mN. In image 7b you can see how the variation in electrical resistance increases as the applied force increases. The sample follows the applied mechanical deformation with excellent repeatability, confirming its possible application in the field of sensors applied to intelligent fabrics.

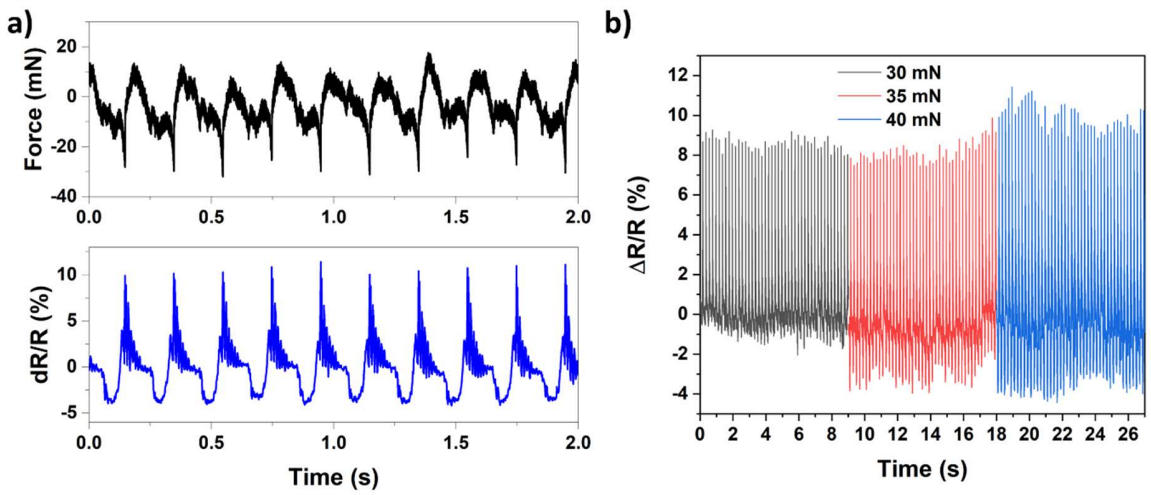

Figure 7. a) Electrical resistance measurements under cyclic compressive stress. The upper part of the graph shows the force applied to the sensor, while the lower part shows the relative electrical resistance variation. b) Electrical response of the sensor when subjected to compressive stresses with different force loads.

Conclusions

In this work the laser graphitization of an aramid yarn for the fabrication of a wearable deformation sensor has been presented. The laser-induced graphene obtained with three different writing approaches was characterized by Raman spectroscopy and electron microscopy to study the structural and morphological properties confirming the few-layer nature of the graphene. Electrical measurements demonstrated the suitable properties for its application in resistive sensing field without a noteworthy degradation of the mechanical performances. A yarn shaped deformation sensor was fabricated and electrically characterized in static and dynamic bending conditions exhibiting up to 120% variation of resistance under bending and about 10% under dynamic solicitation with stable behavior during repeated cycling. These findings confirm the potential application of the described technology for the fabrication of highly performing wearable sensor.

AUTHOR INFORMATION

Corresponding Author

A. Lamberti, Politecnico di Torino, Dipartimento di Scienza Applicata e Tecnologia (DISAT), Corso Duca Degli Abruzzi, 24, 10129 Torino, Italy, email: andrea.lamberti@polito.it

Author Contributions

A.L. was the main researcher working on this project. M.P. and F.C. performed the laser writing of the LIG, S.S. made the mechanical measurements, M.F. performed the electron microscopies, S.B. performed the Raman analysis while L.S. supervised the work. The manuscript writing and data discussion was done by A.L with the help of all authors. All authors have given approval to the final version of the manuscript.

ADDITIONAL INFORMATION

Funding Sources

This project was conducted in the framework of the project Proof of Concept funded by Compagnia di San Paolo (ID 11557).

Supporting Information

Supporting Information is available online or from the author.

Additional FESEM characterizations, optical microscope images, Raman spectra and experimental details.

REFERENCES

1. Ye, R.; James, D. K.; Tour, J. M., Laser-Induced Graphene. *Acc. Chem. Res.* **2018,** *51* (7), 1609-1620.
2. Ye, R.; James, D. K.; Tour, J. M., Laser-Induced Graphene: From Discovery to Translation. *Adv. Mater.* **2019,** *31* (1).
3. Parmeggiani, M.; Zaccagnini, P.; Stassi, S.; Fontana, M.; Bianco, S.; Nicosia, C.; Pirri, C. F.; Lamberti, A., PDMS/Polyimide Composite as an Elastomeric Substrate for Multifunctional Laser-Induced Graphene Electrodes. *ACS Applied Materials and Interfaces* **2019,** *11* (36), 33221-33230.
4. d'Amora, M., Lamberti, A., Fontana, M., & Giordani, S. , Toxicity assessment of laser-induced graphene by zebrafish during development. . *Journal of Physics: Materials,* **2020,** *3* (3), 034008.
5. Zaccagnini, P.; di Giovanni, D.; Gomez, M. G.; Passerini, S.; Varzi, A.; Lamberti, A., Flexible and high temperature supercapacitor based on laser-induced graphene electrodes and ionic liquid electrolyte, a de-rated voltage analysis. *Electrochim. Acta* **2020,** *357*.
6. Han, T.; Nag, A.; Simorangkir, R. B. V. B.; Afsarimanesh, N.; Liu, H.; Mukhopadhyay, S. C.; Xu, Y.; Zhadobov, M.; Sauleau, R., Multifunctional flexible sensor based on laser-induced graphene. *Sensors (Switzerland)* **2019,** *19* (16).
7. Tao, L. Q.; Tian, H.; Liu, Y.; Ju, Z. Y.; Pang, Y.; Chen, Y. Q.; Wang, D. Y.; Tian, X. G.; Yan, J. C.; Deng, N. Q.; Yang, Y.; Ren, T. L., An intelligent artificial throat with sound-sensing ability based on laser induced graphene. *Nature Communications* **2017,** *8*.
8. Ren, M.; Zheng, H.; Lei, J.; Zhang, J.; Wang, X.; Yakobson, B. I.; Yao, Y.; Tour, J. M., CO2to Formic Acid Using Cu-Sn on Laser-Induced Graphene. *ACS Applied Materials and Interfaces* **2020,** *12* (37), 41223-41229.
9. Wang, L.; Fu, X.; He, J.; Shi, X.; Chen, T.; Chen, P.; Wang, B.; Peng, H., Application Challenges in Fiber and Textile Electronics. *Adv. Mater.* **2020,** *32* (5).
10. Jang, Y.; Kim, S. M.; Spinks, G. M.; Kim, S. J., Carbon Nanotube Yarn for Fiber-Shaped Electrical Sensors, Actuators, and Energy Storage for Smart Systems. *Adv. Mater.* **2020,** *32* (5).
11. Lamberti, A.; Gigot, A.; Bianco, S.; Fontana, M.; Castellino, M.; Tresso, E.; Pirri, C. F., Self-assembly of graphene aerogel on copper wire for wearable fiber-shaped supercapacitors. *Carbon* **2016,** *105*, 649-654.
12. Serrapede, M.; Rafique, A.; Fontana, M.; Zine, A.; Rivolo, P.; Bianco, S.; Chetibi, L.; Tresso, E.; Lamberti, A., Fiber-shaped asymmetric supercapacitor exploiting rGO/Fe2O3 aerogel and electrodeposited MnOx nanosheets on carbon fibers. *Carbon* **2019,** *144*, 91-100.
13. Rafique, A.; Massa, A.; Fontana, M.; Bianco, S.; Chiodoni, A.; Pirri, C. F.; Hernández, S.; Lamberti, A., Highly Uniform Anodically Deposited Film of MnO2 Nanoflakes on Carbon Fibers for Flexible and Wearable Fiber-Shaped Supercapacitors. *ACS Applied Materials and Interfaces* **2017,** *9* (34), 28386-28393.
14. Xu, X.; Xie, S.; Zhang, Y.; Peng, H., The Rise of Fiber Electronics. *Angewandte Chemie - International Edition* **2019,** *58* (39), 13643-13653.
15. Kane, F., Shen, J., Morgan, L., Prajapati, C., Tyrer, J., & Smith, E. , Innovative technologies for sustainable textile coloration, patterning, and surface effects. *Sustainability in the Textile and Apparel Industries* **2020**, 99-127.
16. Hu, Y.; Cheng, H.; Zhao, F.; Chen, N.; Jiang, L.; Feng, Z.; Qu, L., All-in-one graphene fiber supercapacitor. *Nanoscale* **2014,** *6* (12), 6448-6451.

17. Gore, P. M.; Kandasubramanian, B., Functionalized Aramid Fibers and Composites for Protective Applications: A Review. *Ind. Eng. Chem. Res.* **2018,** *57* (49), 16537-16563.
18. Ertekin, M.; Erhan Kirtay, H., Cut resistance of hybrid para-aramid fabrics for protective gloves. *Journal of the Textile Institute* **2016,** *107* (10), 1276-1283.
19. Seretis, G. V.; Kostazos, P. K.; Manolakos, D. E.; Provatidis, C. G., On the mechanical response of woven para-aramid protection fabrics. *Composites Part B: Engineering* **2015,** *79*, 67-73.
20. Laurenti, M.; Stassi, S.; Lorenzoni, M.; Fontana, M.; Canavese, G.; Cauda, V.; Pirri, C. F., Evaluation of the piezoelectric properties and voltage generation of flexible zinc oxide thin films. *Nanotechnology* **2015,** *26* (21).